

Review

# Current Trends in the Use of Semiconducting Materials for Electrochemical Aptasensing

Leda Bousiakou <sup>1,\*</sup>, Omar Al-Dosary <sup>2</sup>, Anastasios Economou <sup>3</sup>, Veronika Subjakova <sup>4</sup> and Tibor Hianik <sup>4,\*</sup>

<sup>1</sup> IMD Laboratories Co., R&D Section, Lefkippos Technology Park, National Centre for Scientific Research (NCSR) Demokritos, Agia Paraskevi, 15130 Athens, Greece

<sup>2</sup> Department of Physics and Astronomy, College of Science, King Saud University, P.O. Box 2455, Riyadh 11451, Saudi Arabia; omar@ksu.edu.sa

<sup>3</sup> Department of Chemistry, National and Kapodistrian University, 15771 Athens, Greece; aeconomou@chem.uoa.gr

<sup>4</sup> Department of Nuclear Physics and Biophysics, Faculty of Mathematics, Physics and Informatics, Comenius University, Mlynská dolina F1, 842 48 Bratislava, Slovakia; veronika.subjakova@fmph.uniba.sk

\* Correspondence: leda@imdlaboratories.gr (L.B.); tibor.hianik@fmph.uniba.sk (T.H.)

**Abstract:** Aptamers are synthetic single-stranded oligonucleotides that exhibit selective binding properties to specific targets, thereby providing a powerful basis for the development of selective and sensitive (bio)chemical assays. Electrochemical biosensors utilizing aptamers as biological recognition elements, namely aptasensors, are at the forefront of current research. They exploit the combination of the unique properties of aptamers with the advantages of electrochemical detection with the view to fabricate inexpensive and portable analytical platforms for rapid detection in point-of-care (POC) applications or for on-site monitoring. The immobilization of aptamers on suitable substrates is of paramount importance in order to preserve their functionality and optimize the sensors' sensitivity. This work describes different immobilization strategies for aptamers on the surface of semiconductor-based working electrodes, including metal oxides, conductive polymers, and carbon allotropes. These are presented as platforms with tunable band gaps and various surface morphologies for the preparation of low cost, highly versatile aptasensor devices in analytical chemistry. A survey of the current literature is provided, discussing each analytical method. Future trends are outlined which envisage aptamer-based biosensing using semiconductors.

**Keywords:** DNA aptamers; electrochemical sensors; semiconductors; nanomaterials; carbon materials; metal oxides; conductive polymers; metal organic frameworks



**Citation:** Bousiakou, L.; Al-Dosary, O.; Economou, A.; Subjakova, V.; Hianik, T. Current Trends in the Use of Semiconducting Materials for Electrochemical Aptasensing. *Chemosensors* **2023**, *11*, 438. <https://doi.org/10.3390/chemosensors11080438>

Academic Editor: Boris Lakard

Received: 14 June 2023

Revised: 28 July 2023

Accepted: 3 August 2023

Published: 6 August 2023



**Copyright:** © 2023 by the authors. Licensee MDPI, Basel, Switzerland. This article is an open access article distributed under the terms and conditions of the Creative Commons Attribution (CC BY) license (<https://creativecommons.org/licenses/by/4.0/>).

## 1. Introduction

Aptamers are a category of synthetic single-stranded DNA or RNA oligonucleotides that are currently being investigated as molecular probes for a variety of organic and inorganic target species. They are normally 15–80 nucleotide bases long and are produced via a process termed the Systematic Evolution of Ligands by Exponential Enrichment (SELEX) [1–3]. Aptamers are also coined chemical antibodies as they were initially developed to replace traditional antibodies, but with multiple advantages. Unlike antibodies, which specifically target proteins or other analytes, aptamers have a much wider scope of applications as they can target different ions, heavy metals, organic and inorganic molecules, proteins, viruses, bacteria, or cells. In addition, aptamers are less expensive than antibodies and easy to chemically synthesize, have a small size and flexible structure, and, unlike antibodies, are stable and do not suffer from batch-to-batch variations. Once the aptamer sequence is selected, it can be reproduced with high fidelity [4]. Aptamers are also easily modified with different functional groups or molecules, for instance, redox reporters, such as the organometallic compound ferrocene and the organic dye methylene blue. These probes are commonly attached on one end of the aptamer to facilitate electron transfer in

electrochemical sensing applications [5,6]. The other end of the aptamer can be modified by various groups, such as biotin, -SH (thiol), or -NH<sub>2</sub> (amino) groups, thus allowing its immobilization on various surfaces. An additional advantage of aptamers is their ability to distinguish between molecules closely related to each other, such as conformational isomers, amino acids with mutations in the corresponding DNA sequences, or even targets with different functional groups. Their main difference to antibodies lies in the specific three-dimensional interaction that drives the formation of aptamer–target complexes, as illustrated in Figure 1, that can refold to their original conformation when optimal conditions are restored [7]. Aptamers can fold in secondary structures, such as stems, loops, bulges, pseudoknots, G-quadruplexes, and kissing hairpins, allowing for the detection of the target molecule by utilizing primarily hydrogen bonding and Van der Waals interactions [8].

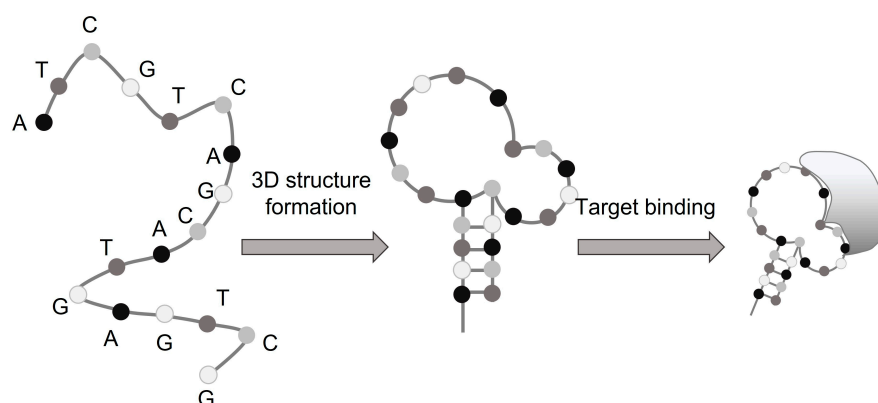


**Figure 1.** The scheme of aptamer functionality. Reproduced from [7].

DNA aptamers are widely used as receptors in various types of biosensors. Among them, electrochemical biosensors are of substantial interest due to the relatively low cost of portable and USB-based potentiostats, their simple preparation, good stability, reproducibility, and uncomplicated data evaluation. Electrochemical aptasensors were first introduced in 2004 as robust, low-cost, fast, multi-analyte devices with excellent potential for miniaturization [9,10]. In recent years, electrochemical aptasensors have been commonly used for the selective and sensitive detection of analytes, such as small molecules, metal-ions, proteins, and cells [11,12]. Currently, several electrochemical detection techniques are being utilized, including amperometry, electrochemical impedance spectroscopy (EIS), potentiometry (such as FET/MOSFETs), as well as voltammetry (including cyclic voltammetry) [13]. Within voltammetry, differential pulse voltammetry (DPV) and square wave voltammetry (SWV) are commonly used due to their capacity to discriminate against capacitive current, providing improved signal recording [14]. One of the most common electrochemical set-ups in this regard is an integrated screen-printed sensing platform, comprising a working electrode (WE), a reference electrode (RE), and a counter electrode (CE). Screen-printed sensors are usually preferred as they reduce the undesired effects of the ohmic drop, decrease sample consumption, allow for higher rates of mass transport, reduce the double layer capacitance, and enhance the signal-to-noise ratio [15,16]. Aptamers can be immobilized on the working electrode via several routes, including physisorption, chemisorption, or by utilizing biocoatings, such as avidin, streptavidin, or neutravidin [17]. In general, the immobilization of the aptamers on the surface of the working electrode is advantageous compared to them being dispersed in solution. It is preferred for lower cost, signal amplification, sensor regeneration, patterning, and long-term storage.

Several materials have been used for fabricating aptamer-based electrochemical sensors, including gold, platinum, carbon, metal oxides, conducting polymers, as well as metal organic frameworks (MOFs) [18], with the bonding of the functional groups being dependent on the type of electrode (e.g., Au-S in gold, -COOH and -NH<sub>2</sub> bond in carbon, graphene oxide, carbon nanotubes, etc.). Semiconductor surfaces have attracted consider-

able interest within the electrochemical community since the landmark study of TiO<sub>2</sub>-based water splitting [19] that elucidated the properties of semiconductor electrolyte surfaces. In addition, transition metal oxides are more suitable for large-scale commercialization compared with noble metals due to their wide availability, low cost, and excellent stability. Oxides of metals such as Ti, Cu, and Zn have been routinely used, allowing for good stability and sensitivity of the respective sensors. For example, TiO<sub>2</sub> surfaces have been routinely used as working electrode materials [20]. These can be produced either as thick or thin films, with their surface morphology manipulated to allow for different roughness, porosity, as well as microscale and nanoscale features unique for various applications. Moreover, they have low toxicity, are biocompatible, and are corrosion-resistant, offering also low fabrication costs. Another feature is that their electron transport properties can be fine-tuned via doping, which in turn can enhance charge transfer. For example, nanostructured TiO<sub>2</sub> surfaces support good electron transport between the bioreceptor and analyte due to the electron-accepting character of TiO<sub>2</sub>. It is known that TiO<sub>2</sub> anatase nanoparticle monolayers show good electronic connectivity with the substrate, allowing for their use as electrode materials. Moreover, anatase thin films show chemical resistance towards moderate acid and alkali solutions, making them suitable for use in electrochemical biosensors.

Moreover, ZnO nanostructured materials exhibit useful properties such as high electrical conductivity, cost-effectiveness, and chemical stability [21,22]. CuO has also been utilized in aptasensing as it offers good electrochemical activity, as well as the ability to stimulate electron transfer reactions at lower potentials. Other metal oxides, such as WO<sub>3</sub> and NiO, have also been used. For example, WO<sub>3</sub> has been used as a semiconducting electrode, showing excellent stability [23]. Furthermore, NiO exhibits a high isoelectric point (Ip), good ionic conductivity, and capacitive action, making it suitable for the electrochemical transduction of DNA-based sensing [24–26].

Other semiconducting candidates for use in electrochemical aptasensing are carbon allotropes [27] with semiconducting properties, such as carbon nanotubes (CNTs), fullerenes—a *n*-type semiconductors, graphene oxide (GO), and reduced graphene oxide (rGO). In particular, the level of conductivity in carbon nanotubes varies with chirality, ranging from metallic ‘armchair’ nanotubes to semiconducting ‘zigzag’ or ‘chiral’ patterns. In general, semiconducting single-walled carbon nanotubes (SWCNTs) are used twice as frequently as metallic ones. Nevertheless, growing SWCNTs of a unique desired chirality have not yet been realized industrially. Finally, biocompatible conjugated polymers, i.e., polymers with a  $\pi$ -conjugated, semiconducting backbone, have also been used for biomolecule immobilization, offering improved electrical conductivity and tailorable transport characteristics for biological applications [28–30]. Some other examples of organic semiconductor materials are 6,13-bis((triisopropylsilyl)ethynyl)pentacene (TIPS-pentacene), regioregular poly(3-hexylthiophene-2,5-diyl), commonly known as P3HT, poly(3,4-ethylenedioxythiophene) polystyrene sulfonate, i.e., PEDOT:PSS, C10-dinaphtho[2,3-b:2',3'-f]thieno[3,2-b]thiophene (DNNT) and C8[1]benzothieno[3,2-b][1]-benzothiophene (BTBT). These materials offer the advantage of low weight, flexibility, and stretchability compared to inorganic semiconductor materials but still exhibit lower conductivity, lower field-effect mobility, lower thermal stability, and lower lifetime. In Table 1, some advantages and disadvantages of the different electrode materials are presented, considering their importance in aptamer immobilization, conductivity, surface morphology, and catalytic effects.

**Table 1.** Comparison of various electrode materials for preparation of electrochemical aptasensors.

Material	Advantages	Disadvantages
Metal system	Excellent electrical conductivity, great chemical stability	Hydrophobic, surface electrons can lead to denaturing of biomolecules
Metal oxides	Low cost, easy to prepare, wide potential window (transition metal oxides), tunable composition, hydrophilic	Lower conductivity, high recombination rate (especially for photoelectrochemical applications)

Table 1. Cont.

Material	Advantages	Disadvantages
WO <sub>3</sub>	Non-stoichiometric properties, good electron transport, stable in acid conditions, moderate hole-diffusion length (approx. 150 nm) especially for photoelectrochemical applications	Unstable at pH > 4
ZnO	Good stability, environmentally friendly, inexpensive, high carrier mobility	ZnO NPs are ion shedding particles and zinc ions can lead to oxidative stress
TiO <sub>2</sub>	Highly stable over a range of pH values in aqueous environments, even under illumination, good electrochemical activity, non-toxic	Low absorption in the visible light (especially for photoelectrochemical applications)
CuO	Good electrochemical activity and the ability to stimulate electron transfer reactions at lower potentials	Potentially toxic effects in the case of CuO nanoparticles
NiO	High isoelectric point, porous morphology, small crystallite size, chemical stability	The charge acceptance at temperatures above 35 °C is not good enough
Conductive polymers	Filming has good flexibility, unique solution processibility, biocompatible	Low conductivity, lower electrochemical stability
Carbon systems	Large specific surface area, high conductivity, electrochemical stability, low cost	Poor dispersity
Graphene	Large specific area, excellent electrical properties, high control on functionalization	Susceptibility to oxidative environments, hydrophobic, high cost
Graphene oxide	High dispersibility in water (hydrophilic), abundant presence of oxygenated groups—binding sites	Lower electrical conductivity, surface random functionalization
Reduced graphene oxide	High electrical conductivity, good control on functionalization, less expensive than graphene	Low density of oxygen containing groups, lower colloidal stability, hydrophobic
Carbon nanotubes	Large surface area, excellent electrical properties	High cost, complex preparation, potential toxic

In the subsequent sections, a working electrode modification will be reviewed towards electrochemical aptasensing based on semiconducting materials or hybrid structures, exploring metal–semiconductor combinations or combinations of different semiconducting platforms.

## 2. Carbon Allotropes within Electrochemical Aptasensing

In general, natural carbon allotropes such as graphite, as well as synthetic ones including fullerenes, carbon nanotubes (CNTs), and graphene, have received significant attention for electrochemical biosensing due to their unique electrical properties and technological importance [31]. Fullerenes exhibit a large surface area that can be appropriately functionalized, as well as strong electron accepting capacity, taking up electrons and releasing them to the transducer [32]. This is due to a 1.8 eV gap between the lowest unoccupied (LUMO) and highest occupied (HOMO) molecular orbitals, as seen in Figure 2.

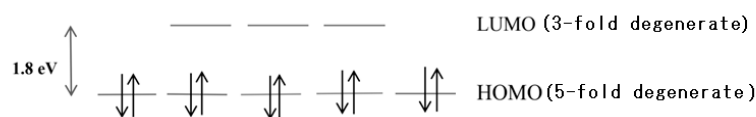
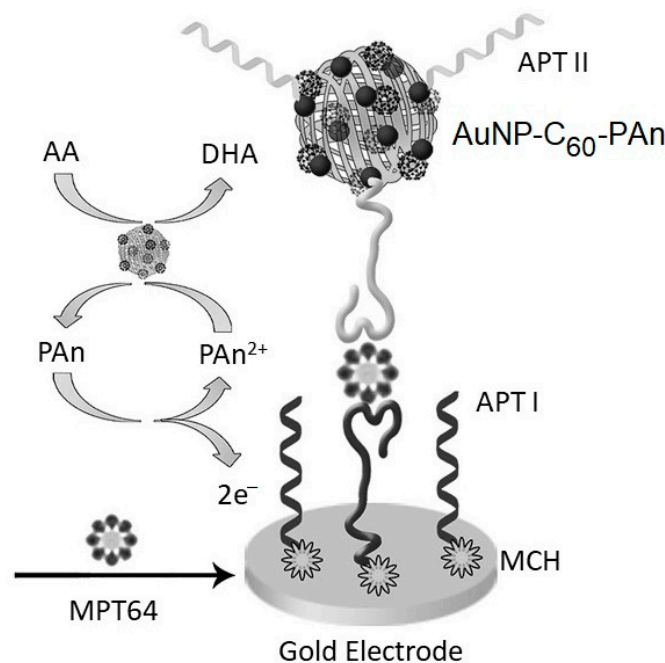


Figure 2. HOMO and LUMO gap in fullerene-C<sub>60</sub>. Reproduced from [33].

Furthermore, while fullerenes, such as the buckminsterfullerenes C<sub>60</sub>, C<sub>70</sub>, and C<sub>80</sub>, have good solubility in non-polar organic solvents, such as toluene and hexane at ~280 K, functionalization with thiol and amino groups leads to enhanced water solubility [34,35].

The first electrodes involving the use of  $C_{60}$  [36] were prepared by drop-casting  $C_{60}$  on carbon electrodes to improve their performance and were then coated with a Nafion film for protection. In general, fullerenes can be modified via the C=C bonds, with  $C_{60}$  having 30 single and 60 aromatic double bonds. As a result, bonds with amino acids, hydroxyl, and carboxyl groups can be readily formed. For example, Cassell et al. [37] studied the interaction between DNA and fullerene using  $C_{60}$ -N,N-Dimethylpyrrolidinium iodide as a complexing agent utilizing the DNA phosphate groups. Moreover, the use of surfactants can prevent DNA/fullerene hybrids from aggregation. The coil-like fullerene  $C_{60}$ , doped by polyaniline ( $C_{60}$ -PAn) nanocomposites, have also been used for the development of aptasensors considering the advantage of their large surface area and excellent electric performance. Using this nanomaterial, an electrochemical aptasensor was proposed for the detection of *Mycobacterium tuberculosis* antigen MPT64, as illustrated in Figure 3 [38]. In this regard, the sandwich reaction of the MPT64 target is utilized between the capture aptamer (APT I) and the tracer label, i.e., the gold nanoparticles (AuNPs) decorated  $C_{60}$ -PAn, i.e., AuNPs- $C_{60}$ -PAn (APT II). The detection signal was then enhanced by the electrochemical oxidation of ascorbic acid (AA) to dehydroascorbic acid (DHA) through the redox nanoprobe  $C_{60}$ -PAn. The sensor allowed for the detection of MPT64 with a limit of detection (LOD) of 20 fg/mL in a linear range of 0.02–1000 pg/mL.



**Figure 3.** Schematic diagram of the preparation of the electrochemical aptasensor for the detection of *Mycobacterium tuberculosis* antigen MPT64. APTI: 5′ -SH-(CH<sub>2</sub>)<sub>6</sub>-TGGGAGCTGATGTCGCATGGG-TTTTGATCACATGA-3′, APTII: 5′ -SH-(CH<sub>2</sub>)<sub>6</sub>-TTCGGGAATGATTATCAAATTATGCC CTCTGAT-3′. Partially reproduced from [38] with the permission of Elsevier.

CNTs have been used along with fullerenes for electrochemical biosensing. CNTs are strong, durable, and lightweight rolled-up graphene sheets, with their chirality determining their electrical properties. Thus, while ‘armchair’ carbon nanotubes are always semiconducting, ‘zig-zag’ ones exhibit higher conductivity. Modifying their surfaces with COOH, -NH<sub>2</sub>, -F, or other groups promotes their dispersion in a variety of solvents and polymers, enabling their wider use. Aptamers can self-assemble on the walls of carbon nanotubes using their nucleic acid bases via  $\pi$ - $\pi$  stacking interactions. This allows for the formation of a hybrid material that has excellent applications in biosensing [39]. An example is illustrated in Figure 4 in which DNA aptamers specific to cellular prions (PrP<sup>C</sup>) are immobilized, via an amide linkage, on the surface of semiconducting multi-walled carbon nanotubes (MWCNTs), whose conductivity varies with chirality [40,41]. This ap-

proach allowed for the development of an electrochemical quartz crystal microbalance (EQCM)-based biosensor for the detection of PrP<sup>C</sup> using aptamers with an LOD of 50 pM. The authors also compared the sensitivity of prion detection using two kinds of monoclonal antibodies, BAR 223 and PRI 308, that bind PrP<sup>C</sup> at different protein regions. The LODs have been comparable with those of aptasensor and reached 20 pM for BAR 223 and 48 pM for PRI 308, respectively [41].

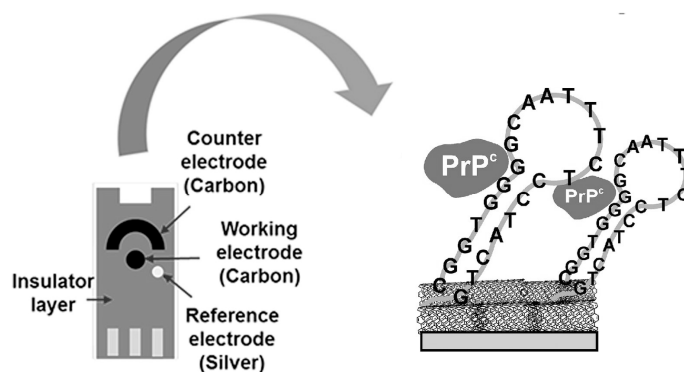


**Figure 4.** Schematic representation of a working electrode based on cellular prions immobilized on carbon nanotubes. Partially reproduced from [41] with the permission of Eureka Science.

In another application, the surface composed of MWCNTs and fourth generation polyamidoamine dendrimers (PAMAM G4) were applied for the development of an electrochemical aptasensor specific to PrP<sup>C</sup> [42]. The prions were detected based on the redox current of ferrocene (Fc) immobilized between the aptamers and the dendrimers. This approach allowed for the detection of PrP<sup>C</sup> in spiked blood plasma with an LOD of 0.5 pM and a dynamic range of 1 pM to 10  $\mu$ M. The recovery was 85% at 1 nM prions. A similar approach, using conducting polypyrrol (PPY) layers at a gold surface for the immobilization of dendrimers and DNA aptamers, allowed for the detection of PrP<sup>C</sup> with an LOD of 0.8 pM (Figure 5). This is lower by a factor of  $10^3$  in comparison with the immobilization of aptamers at flat PPY layers. The electrochemical aptasensor allowed for the detection of cellular prions in spiked blood plasma with recovery of 90% [43].

Recently, carboxylated MWCNTs in a nanocomposite with CoHCF and Au nanoparticles, immobilized on glassy carbon electrodes (GCE), have also been used for the electrochemical detection of interleukin 6 (IL 6), with a linear range of 0.5–1000 pg/mL and an LOD of 0.17 pg/mL [44]. In another study, an electrochemical aptasensor for the detection of adenosine was designed, incorporating MWCNTs decorated with PtCu nanoparticles for signal amplification on a gold electrode. This led to an increase in aptamer immobilization density, improving the signal and leading to a linear range between 10 nM and 1.0  $\mu$ M with an LOD of 1.0 nM [45].

In another work, Zelada-Guillén et al. [46] developed a potentiometric aptasensor utilizing SWCNTs for the detection of *Salmonella typhi* (Figure 6). In sequence, aptamers were chemisorbed on the carboxylated SWCNTs by using a five-carbon amine spacer, i.e., the 1-pentylamine molecule ( $\text{CH}_3(\text{CH}_2)_4\text{NH}_2$ ) and an amine group ( $-(\text{CH}_2)_5\text{NH}_2$ ) at the 3' end. The potentiometric response time of the biosensor was shorter than 60 s, and the working range extended from 0.2 CFU/mL (1 CFU in 5 mL PBS) to  $10^6$  CFU/mL. In this regard, the rapid response time indicates a fast affinity equilibrium between the aptamer and the *Salmonella typhimurium*.

In a different piece of work, Zelada-Guillén et al. [47] utilized SWCNTs again, demonstrating the potentiometric label-free detection and identification of *E. coli* in milk and apple juice, reaching sensitivity as low as 6 CFU/mL and 26 CFU/mL, respectively. Similarly, for the detection of whole-cell *Salmonella Enteritis* and *Salmonella typhimurium* [48], the immobilization of an amino-modified DNA aptamer on a COOH-rich MWCNTs modified ITO electrode was proposed. The preparation was evaluated using voltammetric techniques.

The LODs were 55 CFU/mL for *S. enteritidis* and 67 CFU/mL for *S. typhimurium*. Moreover, Zou et al. [49] prepared an aptasensor for the detection of diclofenac by using a GCE covered by MWCNTs (Figure 7).  $\text{NH}_2$ -terminated aptamers have been covalently attached to the MWCNTs through carboxyl groups activated by EDC/NHS. Upon incubation with the pharmaceutical diclofenac, they achieved an LOD of 162 fM.

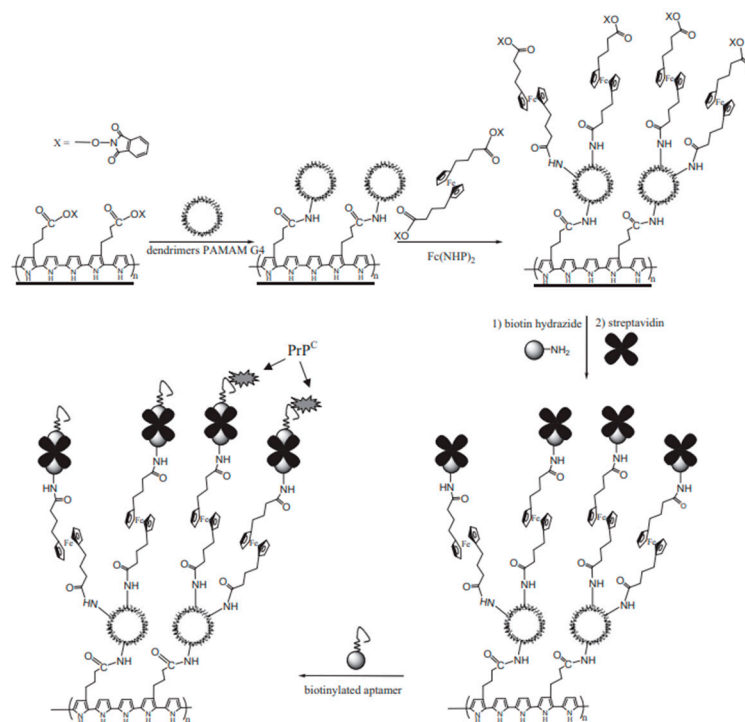


**Figure 5.** The scheme of preparation aptasensor for detection of PrP<sup>C</sup> based on PPY layers and PAMAM G4 dendrimers. The redox probe ferrocene is localized between dendrimers and aptamers. Reproduced from [43] with the permission of Elsevier.

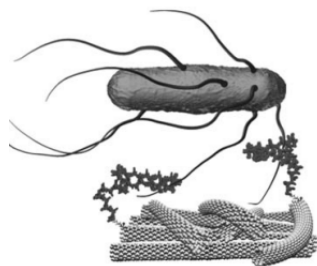


**Figure 6.** Schematic representation of the interaction between *Salmonella typhimurium* and the hybrid aptamer-SWCNTs system. Reproduced from [46] with the permission of Wiley-VCH.

Carbon quantum dots (CQDs) have been studied for both electrochemical and photoelectrochemical biosensing as a promising new class of metal-free, low-cost, nanosized light-harvesters. CQDs are composed of quasi-spherical carbon nanoparticles with sizes below 10 nm and display semiconductor-like properties. CQDs-WS<sub>2</sub>-modified GCE have been prepared with the view to fabricate label-free electrochemical aptasensors for the determination of sulfamethazine [50]. The aptamers were electrostatically adsorbed using cationic polyethyleneimine, and a  $[\text{Ru}(\text{NH}_3)_6]^{3+}$  redox probe was employed. The aptasensors showed a wide linear response between 10 pM and 1.0  $\mu\text{M}$  and a low LOD of 4.0 pM.

Finally, Cheng et al. [51] prepared a photoelectrochemical (PEC) aptasensor for the detection of thrombin using a carboxyl modified aptamer, covalently immobilized on

an ITO electrode, which was sensitized with a photoactive matrix based on  $\text{TiO}_2$  loaded with CQDs. This resulted in a stable aptasensor with a linear response between 1.0 and 250 pM and an LOD of 0.83 pM. An interesting approach has been discussed by Kulikova et al. [52] that prepared an electrochemical aptasensor for the detection of kanamycin. In this work, a  $-\text{NH}_2$  modified DNA aptamer mixed with an oligolactide derivative of thiacalix[4]arene in a cone configuration was immobilized on a glassy carbon electrode modified with carbon black in a chitosan matrix. The LOD was determined to be 0.3 nM, while the method was validated in spiked milk and yogurt samples with recovery rates of over 90%. Aptasensors based on carbon nanomaterials have been extensively reported also in the review by Evtugyn et al. [17].

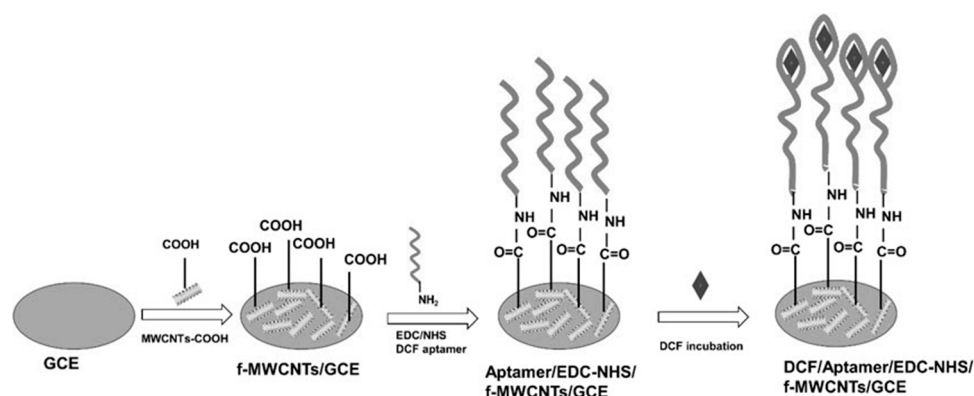


**Figure 7.** Immobilization of aptamers on the carboxyl functionalized MWCNTs for diclofenac detection. Reproduced from [49].

As can be concluded from this overview, carbon nanomaterials have a great advantage in the development of electrochemical aptasensors. The surface of electrodes modified with MWCNTs is characterized by a larger effective area in comparison to flat electrodes. This allows for an increase in the surface density of the aptamers using carbodiimide chemistry for their immobilization through the interaction between amino-modified aptamers and activated  $-\text{COOH}$  groups at the surface of carbon nanotubes. These structures allow for the preparation of the sensors based on various nanocomposites such as MWCNTs-dendrimers and those doped by redox probes such as Fc. As it has been shown above, the MWCNTs-dendrimer composite with immobilized aptamers and Fc allowed for a substantial increase in the sensitivity of the detection cellular prions in comparison with flat layers based on conducting polymers, such as PPY. Further comparison of the properties of electrochemical aptasensors based on carbon nanomaterials for selected analytes is shown in Table 2.

### 3. Inorganic Metal-Oxide-Based Semiconductors

Both inorganic and organic semiconductor materials have been successfully utilized in electrochemical biosensing, including metal oxide semiconductors, polymers with semi-conducting backbones, conjugated polymers, and polymers semiconducting dyes. A comparison between organic and inorganic semiconductors, with their respective advantages and limitations, is made in Figure 8.

In general, metal oxide materials are highly competitive in the field of biosensor based on their versatile morphologies, such as nanosheets, nanorods, flower-like particles, or nanowires and their chemical stability [53,54]. Moreover, they can be easily prepared via several cost-effective methods, including sol-gels, sonochemical precipitation, chemical etching, and hydrothermal approaches. In addition, metal oxides have excellent physico-chemical properties and can combine in composite structures [55]. Several semiconductors, especially  $\text{TiO}_2$  and  $\text{ZnO}$ , have attracted considerable attention due to their low toxicity and sensitivity in electrochemical sensing. Other examples include  $\text{CuO}$ ,  $\text{NiO}$ , and  $\text{WO}_3$  [56]. The major functionalization routes have been both based on electrostatic interactions as

well as covalent bonding. Within aptasensing, a combination of metal oxides with other metals or carbon allotropes has been routinely used [57].

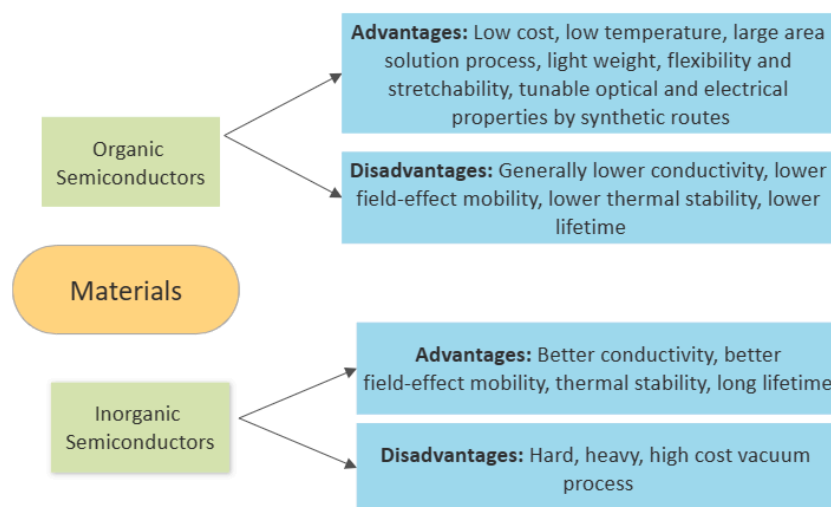


**Figure 8.** Comparison between organic and inorganic semiconductors.

Nadzirah et al. [58] used TiO<sub>2</sub> NPs for the preparation of DNA sensors for *E. coli* detection. The single-stranded (ssDNA) carboxylated probes were immobilized using (3-aminopropyl) triethoxysilane (APTES). The biosensor showed high sensitivity for the detection of a complementary DNA strain from *E. coli* O157:H7 at concentrations as low as 0.1 pM of DNA in bacterial lysates with high specificity and reproducibility. Karimipour et al. [59] used TiO<sub>2</sub> NPs, alone or in combination with rGO, to explore synergistic effects for the adsorption of aptamers for the detection of prostate-specific antigen (PSA). It has been shown that GCE modified with a rGO-TiO<sub>2</sub> nanocomposite exhibited the best performance leading to a stable aptasensor with an LOD of 29.4 fM. In another work by Muniandy et al. [60], a rGO-TiO<sub>2</sub> nanocomposite resulted in a stable aptasensor configuration, allowing for the detection of *Salmonella enterica serovar typhimurium* with a linear range of 10 to 10<sup>8</sup> CFU/mL and an LOD of 10 CFU/mL.

Moreover, Zhang et al. [61] introduced an electrochemical aptasensor based on gold electrodes coated by hollow TiO<sub>2</sub> spheres and a polyacrylic acid (PPAA) for the detection of lysozyme (Figure 9). The abundance of carboxyl groups, along with the large surface area of TiO<sub>2</sub>@PPAA composite, allowed for the effective immobilization of aptamers. Using electrochemical impedance spectroscopy (EIS), it has been possible to detect lysozyme with an LOD of 0.015 ng/mL (1.04 pM) within a range of 0.05–100 ng/mL. For comparison, earlier work on the development of the aptasensor for lysozyme detection reported by Erdem et al. [62] using GCE modified by chitosan-GO composite was less sensitive, with an LOD of 28.5 nM.

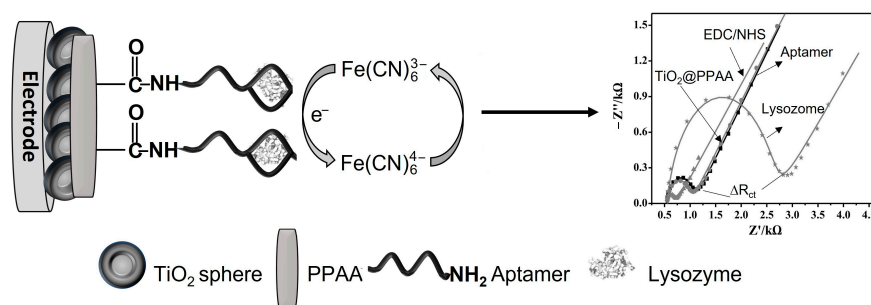


**Figure 9.** Schematic representation of biosensor based on TiO<sub>2</sub>@PPAA for detection of lysozyme. Reproduced from [61] with the permission of Elsevier.

Finally, Au-TiO<sub>2</sub> nanorod arrays have been used on a conductive FTO substrate for the electrochemical detection of adenosine. This array allowed for the attachment of many Au nanoparticles, enhancing aptamer immobilization and improving the redox signal, allowing for an LOD of 0.42 fM to be achieved [63].

Other metal oxides, such as ZnO nanorods, have also been used for the aptasensing of thrombin using ferricyanide ions as a redox marker [64]. In particular, the 30 mer aptamers were electrostatically adsorbed. Upon the detection of thrombin, the aptamer-thrombin complexes slowed down the diffusion of the ferricyanide ions through the surface layer, leading to a decrease in the peak current and charge transfer resistance. At optimum conditions, the LOD was measured to be 3 pM for EIS measurements and 10 pM for CV measurements. Other examples include the use of Au-ZnO nanocomposites immobilized on the surface of a GCE for the detection of the mycotoxin ochratoxin A (OTA) in beverages, such as wine and beer. In particular, the single-stranded SH-modified DNA (cDNA) has been chemisorbed on the Au-ZnO composite. The aptamers—sensitive to OTA that contain complementary bases—were hybridized with cDNA. The redox probe methylene blue (MB) that intercalates between bases has been used as a probe. The formation of OTA-aptamer complexes resulted in the dissociation of aptamers from the surface, and hence the reduction in MB was less effective. This resulted in a decrease in the current measured by DPV. The sensor demonstrated a linear range of OTA detection between 0.1 pg/mL and 30 ng/mL, with an LOD of 0.05 pg/mL [65].

Furthermore, Rahimi et al. [66] chemisorbed amino-modified DNA aptamers on a GCE modified by a Cu<sub>2</sub>O carbon quantum dot nanocomposite (CQD-Cu<sub>2</sub>O) for the detection of wheat flour aflatoxin B1 (Figure 10). An LOD of  $0.9 \pm 0.04$  ag/mL was found with acceptable reproducibility and good stability. However, such a high sensitivity is not typical for electrochemical aptasensors. Moreover, because the constant of dissociation, K<sub>d</sub>, for aptasensors is typically in the range of nM-μM, the aptamer-analyte complex is much less stable below analyte concentrations related to K<sub>d</sub> values.

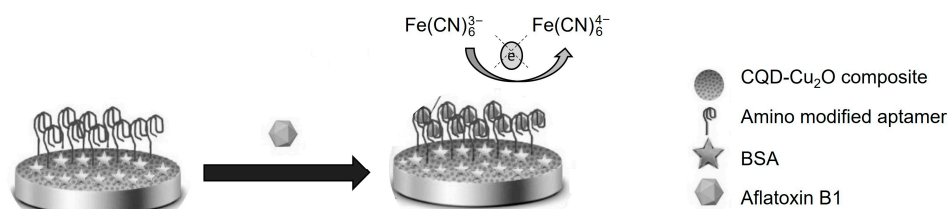


**Figure 10.** Scheme of construction and performance stages of aptasensor for detection of aflatoxin B1. Reproduced from [66] with the permission of Elsevier.

Another electrochemical aptasensor was prepared for the detection of tetracycline [23] based on WO<sub>3</sub>-modified MWCNTs electrodeposited on GCE at the presence of AuNPs. This in turn was functionalized with thiolated DNA aptamers through chemisorption. The MWCNTs-WO<sub>3</sub>@AuNPs allowed for an increase in the conductivity of the sensing layer. The aptasensors showed excellent selectivity in the presence of coexisting antibiotics with a linear range of (0.1–100 nM) and a low LOD of 48 pM.

Finally, an aptasensor for the detection of progesterone of human serum samples was prepared using a carbon quantum dot-NiO-Au nanofiber architecture in combination with MWCNTs on a carbon electrode [25]. This provided a carboxyl-rich immobilization matrix for the immobilization of aptamers. The aptamer-progesterone conjugates led to a decrease in the redox peak current in the presence of [Fe(CN)<sub>6</sub>]<sup>3-/4-</sup> with an increasing progesterone concentration as a result of the hindered electron transfer on the sensing interface. Using DPV, the aptasensors exhibited a dynamic range concentration from 0.01 nM to 1.0 μM and an LOD of 1.86 pM.

Thus, inorganic metal oxide materials, such as TiO<sub>2</sub>, ZnO, NiO, Cu<sub>2</sub>O, or WO<sub>3</sub> in a combination of carbon materials, mostly MWCNTs or carbon quantum dots, allow for a substantial increase in the conductivity of the sensing layers. Nanocomposites containing

MWCNTs or AuNPs have the advantage of being easily functionalized by DNA aptamers through carbodiimide chemistry or chemisorption, respectively. See also Table 2 for a comparative analysis of the aptasensor properties.

#### 4. Other Inorganic Semiconductors (PbS, CdS, ZnS, CdTe)

Other semiconducting materials, such as PbS, CdS, ZnS, and CdTe semiconducting quantum dots (QDs), have been utilized in electrochemical aptasensing, but primarily as aptamer redox tags (Figure 11) frequently encapsulated in metal organic frameworks (MOFs), such as PbS@ZIF-8 and CdS@ZIF-8 [56,67].

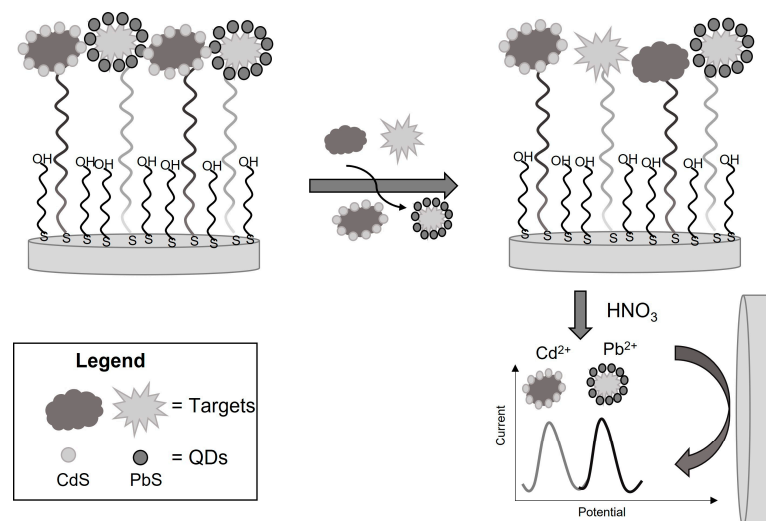


**Figure 11.** General sensing mechanism of electrochemical aptasensors based on quantum dots. Reproduced from [67].

For their successful application, they must possess stability and high reversibility of the redox process, as well as an appropriate potential window, depending on the composition of the working electrode. The application of MOFs in an aptamer-based biosensor was recently reviewed by Evtugyn et al. [68].

Hansen et al. [69] demonstrated the use of CdS and PbS QDs for the simultaneous detection of both thrombin and lysozyme proteins via electrochemical stripping voltammetry. In this work, the thiolated aptamers were chemisorbed at the gold surface. The addition of the thrombin and lysozyme decorated by CdS and PbS QDs, respectively, resulted in stripping voltammetry peaks that were well resolved for the respective QDs and served as the sensing signal. This approach allowed for the detection of these proteins with an LOD of 0.5 pM, which is much lower than previously reported electrochemical aptasensors.

QDs based on semiconductor materials are of high advantage in the development of electrochemical aptasensors. Along with high sensitivity, they also allow for the simultaneous detection of several analytes using stripping voltammetry that can discriminate the analyte by means of their well-resolved voltametric peaks.

#### 5. Organic Semiconductors

Organic semiconductors are excellent candidates for electrochemical biosensing due to their versatile chemical behavior, as well as ease of synthesis for numerous applications [30,70]. Conjugated polymers (CPs) offer high electrical conductivity, tunable charge transport properties, as well as flexible modification. Furthermore, they can provide the basis for wearable and smart skin biosensing devices as they can be designed to provide both flexibility (bending, twisting, and folding) as well as stretchability, with a tensile strain ( $\epsilon$ ) of at least 10%. The CPs used in sensors are mostly PPY, polyaniline (PANI), and polythiophene, as well as poly(3,4-ethylenedioxythiophene):poly(styrene sulfonate) (PEDOT:PSS), which has the highest conductivity amongst solution-processed polymers [71].

CPs are often produced as thin films by chemical or electrochemical synthesis [72]. Within the field of electrochemical aptasensing, several devices have been prepared using organic polymers. A conductive paper-based impedimetric aptasensor was prepared for the detection of carcinoembryonic antigens (CEAs) both in spiked buffer solutions and human serum [73]. For this purpose, the paper was modified using graphene ink and poly (3,4-ethylenedioxythiophene):poly(styrenesulfonate) (PEDOT:PSS) using a simple and continuous coating process, while APTES, succinic anhydride, and bovine serum albumin (BSA) were used for the aptamer immobilization, as can be seen in Figure 12. This resulted in an LOD of 0.45 ng/mL and 1.06 ng/mL in both types of samples, respectively.

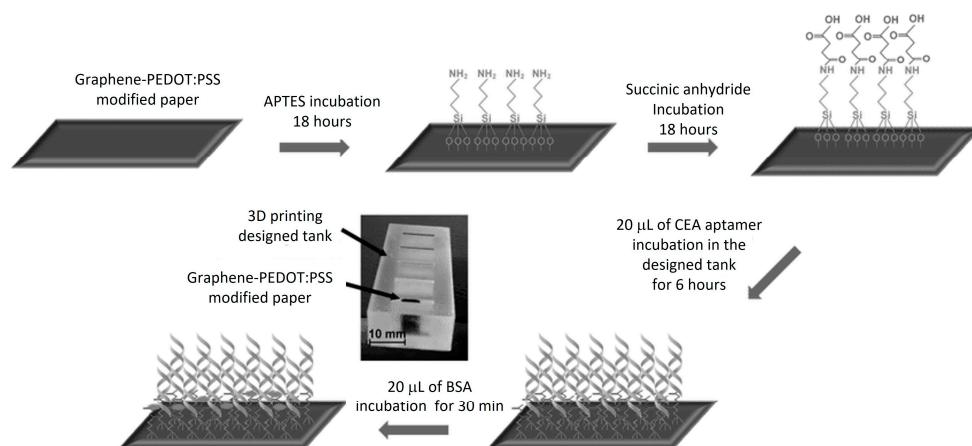


**Figure 12.** Surface functionalization process of the conductive paper-based electrochemical aptasensor. Reproduced from [73].

Another label-free electrochemical aptasensors for the detection of dopamine [74] was prepared on a graphene–polyaniline (GR-PANI) nanocomposite film that allowed for the immobilization of aptamers with phosphate groups at the 5' end via phosphoramidate bonds utilizing the amino groups of the substrate (Figure 13). Using  $[\text{Fe}(\text{CN})_6]^{4-/3-}$  as a redox probe, SWV was utilized, leading to a linear response of 0.007–90 nM and an LOD of 1.98 pM. The electrochemical aptasensor was successfully tested in human serum samples.

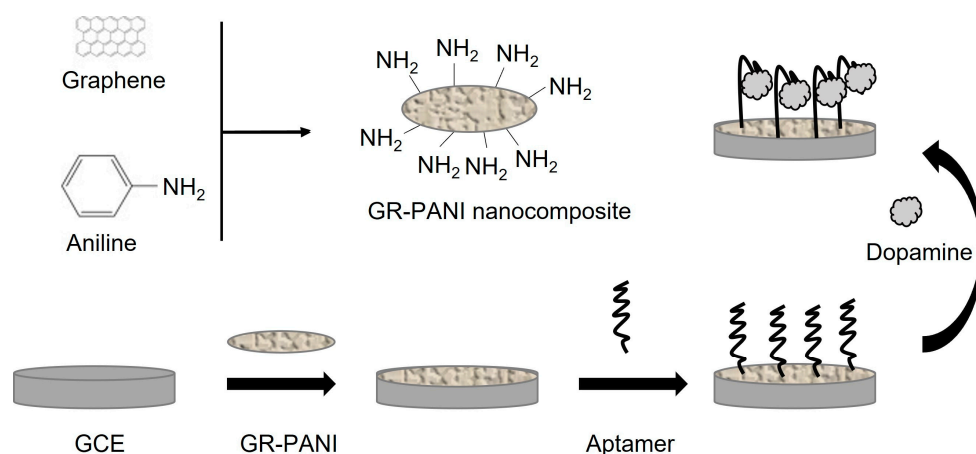


**Figure 13.** Schematic illustration of the dopamine electrochemical aptasensor based on GR-PANI nanocomposites film. Reproduced from [74] with the permission of Elsevier.

For the application of electrochemical aptasensors in a real sample, it is important to focus on the development of surfaces with antifouling properties. This has been demonstrated in the paper by Jolly et al. [75]. They developed an aptasensor for the detection of a prostate cancer biomarker AMACR/P504S using aptamers immobilized at the gold

electrode covered by a PPy-polyethylene glycol (PEG) layer, providing antifouling properties. The PEG carboxyl groups served for the immobilization of the aptamer complexes composed of the  $N\alpha,N\alpha$ -Bis(carboxymethyl)-L-lysine ANTA/ $Cu^{2+}$  redox complex. The aptamer-AMACR/P504S interactions were detected by SWV via the copper redox signal variations. The LOD was 0.15 fM and 1.4 fM in spiked buffer and human plasma samples, respectively.

It is worth noting that the functionalization of organic semiconductors with amine groups improves biocompatibility towards sensor implants because of the cationic charging around the amine group. In particular, Šafaříková et al. [76] evaluated the biocompatibility of a variety of organic/polymer semiconductors, such as P3HT, TIPS-pentacene, PEDOT:PSS, and 3,6-Bis(5-(benzofuran-2-yl)thiophen-2-yl)-2,5-bis(2-ethylhexyl)pyrrolo[3,4-c]pyrrole-1,4(2H,5H)-dione, i.e., DPP(TBFu)<sub>2</sub>, in terms of their stability and cell adhesion, concluding that all materials were stable in aqueous media with sufficient protection, while their ability for cell adhesion could be improved via the self-assembled deposition of collagen IV.

Other electroactive copolymers such as 3,4-ethylenedioxythiophene (EDOT) and 2,2-(3,4-dihydro-2H-thieno[3,4-b][1,4]dioxepine-3,3-diyl)diacetic acid (ProDOT(COOH)<sub>2</sub>) can be used for the immobilization of the amino-modified aptamers to their carboxylic groups. This approach has been reported by Haya et al. [77] for the development of an electrochemical aptasensor for the detection of the MUC1 cancer marker. The aptasensor allowed for the electrochemical detection of MUC1 with an LOD of 418 fM and a linear range of 709 fM to 7.09 nM. The sensor has been stable for 6 days and detected MUC1 selectively in comparison with other proteins such as IgG.

The electropolymerization of several organic dyes, such as methylene blue (MB), azure A and B, or neutral red, can be used for the preparation of redox polymers with semiconducting properties that can improve the sensitivity of electrochemical biosensors [78–80]. For example, neutral red (NR) redox polymer polycarboxylated pillar[5]arene composite prepared on a surface of GCE has been used for the development of an aptasensor for the detection of the aflatoxin AFM1 [79] (Figure 14). AFM1 induced a decrease in the cathodic peak related to the neutral red that served as a probe.



**Figure 14.** The scheme of an aflatoxin M1 aptasensor based on electropolymerized neutral red (NR) at presence of pillar[5]arene (P[5]A-COOH). The  $NH_2$ -modified DNA aptamers specific to aflatoxin M1 (AFM1) were covalently attached to the carboxylic group of P[5]A-COOH activated by carbodiimide chemistry. Adopted from [79] with the permission of Wiley-VCH.

The aptasensor allowed for the detection of AFM1 with an LOD of 0.5 ng/L. The electrochemical aptasensor was validated in spiked milk samples and allowed for the detection of AFM1 in a range of 40–160 ng/kg, which is below the maximal residue limit (MRL) established by EU (50 ng/kg). Additionally, an electrochemical DNA sensor for the detection of the chemotherapeutic drug idarubicin was reported [80]. In this work, DNA from fish sperm with incorporated MB was immobilized at the electropolymerized layers of Azure B at the surface of GCE (Figure 15). The MB produces a well-resolved redox peak that is affected by doxorubicin. This highly sensitive biosensor allowed for the detection of the idarubicin with an LOD of 0.3 fM. While this is not strictly an aptasensor but a DNA sensor, the approach based on the combination of the polymerized layer with MB is rather useful for sensor development.

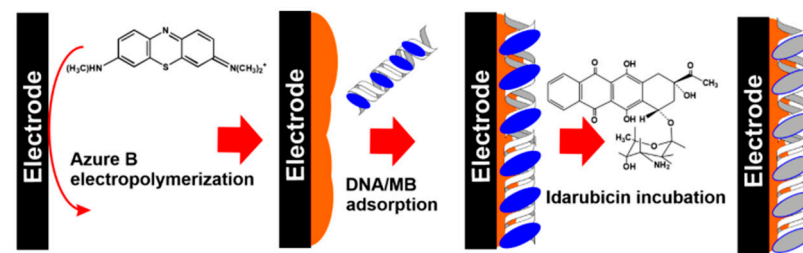


**Figure 15.** The scheme of DNA sensor based on electropolymerized layers of Azure B with entrapped DNA-MB complexes for detection of idarubicin. Adopted from [79].

**Table 2.** Comparison of the properties of the electrochemical aptasensors based on semiconductor materials for the detection of selected analytes.

Analyte	Sensing Surface	Detection Method	LOD	Linear Range	References
Carbon-Based Nanomaterials					
MPT64 antigen	GNPs/C 60/PAN	DPV	20 fg/mL	0.02–1000 pg/mL	[38]
PrP <sup>C</sup>	MWCNTs	EQCM	50 pM	0.1–5 nM	[41]
PrP <sup>C</sup> (103–230)	GE/MWCNTs/PAMAM G4	CV	0.5 pM	1–10 $\mu$ M	[42]
PrP <sup>C</sup> (103–231)	GE/PPY/PAMAM G4	CV	0.8 pM	1–10 $\mu$ M	[43]
Interleukin 6 (IL-6)	GCE/MWCNTs/CoHCF/AuNPs	DPV	0.17 pg/mL	0.5–1000 pg/mL	[44]
Adenosine	SPGE/PtCu/MWCNTs	CV	1 nM	10 nM–1 $\mu$ M	[45]
<i>Escheria coli</i>	GCE/SWCNTs	Potentiometry	6 CFU/mL (Milk); 26 CFU/mL (Juice)	4–10 <sup>4</sup> CFU/mL	[47]
<i>Salmonella typhimurium</i>	GCE/SWCNTs	Potentiometry	1 CFU/mL	0.2–10 <sup>3</sup> CFU/mL	[46]
<i>Salmonella typhimurium</i>	MWCNTs/ITO	EIS	55 CFU/mL	55–5.5 $\times$ 10 <sup>6</sup> CFU/mL	[48]
<i>Salmonella enteritidis</i>	MWCNTs/ITO	EIS	67 CFU/mL	67–6.7 $\times$ 10 <sup>5</sup> CFU/mL	[48]
<i>Salmonella typhimurium</i>	GCE/rGO/CNTs	DPV	10 CFU/mL	10–10 <sup>8</sup> CFU/mL	[81]
<i>Salmonella</i> ATCC 50761	GCE/rGO/MWCNTs	EIS	25 CFU/mL	75–7.5 $\times$ 10 <sup>5</sup> CFU/mL	[82]
Thrombin	ITO/TiO <sub>2</sub> /CQDs	Photocurrent	0.83 pM	1–250 pM	[51]
Myoglobin	SPE/rGO/CNTs	CV	0.34 ng/mL	1 ng/mL–4 $\mu$ g/mL	[83]
Lysozyme	MWCNTs-N-CQDs-chitosan/GCE	DPV	4.26 fM	1 fM–100 nM	[84]
Diclofenac	GCE/MWCNTs	EIS	162 fM	250 fM–1 pM	[49]
Sulfamethazine	GCE/CQDs/WS <sub>2</sub>	DPV	4 pM	10 pM–1 $\mu$ M	[50]
Kanamycin	GCE/CB/Chitosan/Oligolactide	EIS	0.3 nM	0.7–50 nM	[52]
Oxytetracycline	MWCNTs/AuNPs/CS/AuNPs/rGO/AuNPs	DPV	30 pM	1–540 nM	[85]
Inorganic Metal-Oxide-Based Semiconductors					
<i>Escherichia coli</i> O157:H7	IDEs/TiO <sub>2</sub>	Amperometry	0.1 pM	1 pM–10 $\mu$ M	[58]
<i>Salmonella typhimurium</i>	GCE/TiO <sub>2</sub> /rGO	DPV	10 CFU/mL	10–10 <sup>8</sup> CFU/mL	[60]
<i>Staphylococcus aureus</i>	FTO/g-C <sub>3</sub> N <sub>4</sub> /NiO	PEC	24 CFU/mL	10 <sup>2</sup> –10 <sup>6</sup> CFU/mL	[24]
Lysozyme	GE/TiO <sub>2</sub> @PPAA	EIS	0.015 ng/mL	0.05–100 ng/mL	[61]
PSA	GCE/TiO <sub>2</sub> (200)/rGO	EIS	1 pg/mL	0.003–1000 ng/mL	[59]
MUC1	TiO <sub>2</sub> NT/aptamer/c-DNA@QD	Photocurrent	0.52 nM	0.002–0.2 $\mu$ M	[86]
BRCA1 gene	Insulin stabilized Ag–Au@nanoclusters	FET	3 aM	10 aM–1 nM	[87]

Table 2. Cont.

Analyte	Sensing Surface	Detection Method	LOD	Linear Range	References
Progesterone	SPCE/GQDs/NiO/AuNFs/f-MWCNTs	DPV	1.86 pM	0.01–1000 nM	[25]
Adenosine	FTO/TiO <sub>2</sub> /AuNPs	SWV	0.42 fM	1 fM–100 nM	[63]
Thrombin	GE/ZnO	EIS/CV	3 pM/10 pM	3 pM–100 nM	[64]
Thrombin	Sb-doped BaSrFeO <sub>3-δ</sub>	CV	0.02 pM	0.05 pM–0.3 nM	[88]
Thrombin, Lysozyme	GE/CdS/PbS QDs	SWV	20 ng/mL	20–500 ng/mL	[69]
Troponin I	SPCE/3DLSG_MoS <sub>2</sub> _Ag NPs-2.0 hybrid	EIS	0.1 fM	10 <sup>-16</sup> –10 <sup>-10</sup> M	[89]
Ochratoxin A	GCE/ZnO/AuNPs/Nafion	DPV	0.05 pg/mL	0.1–30 × 10 <sup>3</sup> pg/mL	[65]
Aflatoxin B1	GCE/CQDs/Cu <sub>2</sub> O	DPV	0.9 Ag/mL	3 Ag/mL–1.9 µg/mL	[66]
Tetracycline	GCE/MWCNTs/WO <sub>3</sub> @AuNPs	DPV	48 pM	0.1 nM–100 nM	[23]
Kanamycin	PE/MWCNTs@TiO <sub>2</sub> /Thi	ECL	0.049 ng/mL	0.1–10 <sup>5</sup> ng/mL	[90]
Organic Semiconductors					
Carcinoembryonic antigens	PE-graphene/PEDOT:PSS	EIS	0.45 ng/mL	0.77–14 ng/mL	[73]
Dopamine	GCE/GR/PANI	SWV	1.98 pM	0.007–90 nM	[74]
Prostate cancer marker AMACR/P504S	PPy/PEG	SWV	0.15 fM	1 fM–100 nM	[75]
MUC1	EDOT/ProDOT(COOH) <sub>2</sub>	CV	418 fM	709 fM–7.09 nM	[77]
Aflatoxin M1	GCE/NR@pillar[5]arene (P[5]A-COOH)	EIS	0.5 ng/L	5–120 ng/L	[79]
Idarubicin	GCE/Azure B	EIS	0.3 fM	1 fM–100 nM	[80]
Idarubicin	GCE/Azure B	CV	0.3 fM	1 fM–0.1 nM	[80]

3D LSG—lignin derived graphene; AuNFs—gold nanoflowers; BRCA1—breast cancer gene marker; C<sub>60</sub>-fullerene, CNTs—carbon nanotubes; CoHCF—cobalt hexacyanoferrate; CQDs—carbon quantum dots; CS—chitosan; CV—cyclic voltammetry; GNPs/AuNPs—gold nanoparticles; CB—carbon black; DPV—differential pulse voltammetry; ECL—electrochemiluminescence; EDOT/ProDOT(COOH)<sub>2</sub>-3,4-ethylenedioxythiophene and 2,2-(3,4-dihydro-2H-thieno[3,4-b][1,4]dioxepine-3,3-diyl)diacetic acid; EIS—electrochemical impedance spectroscopy; EQCM—electrochemical quartz microbalance; FET—field effect transistor; FTO—fluorine-doped SnO<sub>2</sub> glass; g-C<sub>3</sub>N<sub>4</sub>—carbon nitride; GE—gold electrode; GO—graphene oxide; GR—PANI—graphene-polyaniline; IDEs—interdigitated electrodes; ITO—indium tin oxide; MOFs—metal-organic frameworks; MoS<sub>2</sub>—molybdenum disulphide; MUC1—mucin 1; MWCNTs—multi-walled carbon nanotubes; NR—neutral red; NiO—nickel oxide; PAMAM G4—polyamidoamine dendrimers 4th generation; PAN—polyaniline; PE—paper electrode; PEG—polyethylene glycol; PEC—photoelectrochemical current; PEDOT:PSS—poly(3,4-ethylenedioxythiophene):poly(styrenesulfonate); PGE—pencil graphite electrode; PAA—polyacrylic acid; PPy—polypyrrole; PrP<sup>C</sup>—cellular prion; PSA—prostate-specific antigen; QD—quantum dot; rGO—reduced graphene oxide; SPCE—screen-printed carbon electrode; SWCNTs—single-walled carbon nanotubes; SPE—screen-printed electrode; SWV—square wave voltammetry; Thi—thionin; TiO<sub>2</sub>—titanium dioxide; TiO<sub>2</sub>NT—titanium dioxide nanotube; WS<sub>2</sub>—tungsten disulfide; WO<sub>3</sub>—tungsten trioxide; ZnO—zinc oxide.

It has been demonstrated that organic semiconductor-based nanomaterials are highly advantageous in enhancing the sensitivity of monitoring aptamer–ligand interactions. Especially useful are those doped by redox probes such as methylene blue, ferrocene, or electropolymerized layers with redox properties. Table 2 summarizes the basic properties of the electrochemical aptasensors reviewed. As it can be seen, plenty of semiconductor materials were used for the development of electrochemical aptasensors for several compounds, including small molecules such as antibiotics, hormones, cancer markers, anticancer drugs, proteins, and bacteria. It is rather difficult to make a certain comparison of the effectivity of the semiconductor materials for the detection of a particular analyte. However, all the materials are characterized by high conductivity and high sensitivity. For antibiotics, the sensitivity is at the pM level, which is more than sufficient for a practical application considering that MRL in food for various antibiotics is much higher and is typically in the

nM– $\mu$ M range [91]. Rather high sensitivity has been reached for the detection of bacteria, in the range of 1–10 CFU/mL in certain cases.

## 6. Conclusions

Aptasensors have attracted substantial interest for electrochemical biosensing as an environmentally friendly and cost-effective approach for detecting the analytes of clinical, nutritional, and environmental interest. Aptasensors have the potential for high sensitivity and selectivity in target recognition, being able to even differentiate the chirality of a molecule and its secondary structure. Moreover, the ability of DNA aptamers to regenerate over several detection cycles allows for their incorporation in reusable electrochemical devices. This advantage, in combination with the use of highly versatile, low-cost semiconducting platforms for point of care (POC) diagnostics has become an increasingly popular research area. Nevertheless, there are still drawbacks within electrochemical aptasensing, including the fact that there are still biomarkers for which suitable aptamers have not yet been identified. In addition, aptamers are relatively sensitive to their environment, including salt content and pH, that can affect both the aptamer structure and interaction with the target molecule, thus careful fine-tuning for the aptasensor construction is required. In this regard, further intensive research is required to overcome technical limitations that slow down the progression of novel electrochemical aptasensing platforms for POC or other applications. In addition, for the practical application of aptasensors, it is necessary to focus also on the development of surfaces with antifouling properties to apply the sensors to real complex samples without pretreatment requirements.

**Author Contributions:** Conceptualization, L.B., A.E. and T.H.; formal analysis, L.B., O.A.-D., A.E., V.S. and T.H.; funding acquisition, L.B., A.E. and T.H.; project administration, L.B. and T.H. writing—original draft, L.B., O.A.-D., A.E. and T.H.; writing—review and editing, L.B., O.A.-D., A.E., V.S. and T.H. All authors have read and agreed to the published version of the manuscript.

**Funding:** This work was funded under European Union’s Horizon 2020 research and innovation program through the Marie Skłodowska-Curie grant agreement No. 101007299 and by Science Agency VEGA, project No. 1/0445/23 (to T.H.).

**Institutional Review Board Statement:** Not applicable.

**Informed Consent Statement:** Not applicable.

**Data Availability Statement:** Not applicable.

**Conflicts of Interest:** The authors declare no conflict of interest.

## References

1. Zhuo, Z.; Yu, Y.; Wang, M.; Li, J.; Zhang, Z.; Liu, J.; Wu, X.; Lu, A.; Zhang, G.; Zhang, B. Recent advances in SELEX technology and aptamer applications in biomedicine. *Int. J. Mol. Sci.* **2017**, *18*, 2142. [[CrossRef](#)] [[PubMed](#)]
2. Tuerk, C.; Gold, L. Systematic evolution of ligands by exponential enrichment: RNA ligands to bacteriophage T4 DNA polymerase. *Science* **1990**, *249*, 505–510. [[CrossRef](#)]
3. Ellington, A.D.; Szostak, J.W. In vitro selection of RNA molecules that bind specific ligands. *Nature* **1990**, *346*, 818–822. [[CrossRef](#)]
4. Arshavsky-Graham, S.; Heuer, C.; Jiang, X.; Segal, E. Aptasensors versus immunosensors—Which will prevail? *Eng. Life Sci.* **2022**, *22*, 319–333. [[CrossRef](#)] [[PubMed](#)]
5. Kang, D.; Zuo, X.; Yang, R.; Xia, F.; Plaxco, K.W.; White, R.J. Comparing the properties of electrochemical-based DNA sensors employing different redox tags. *Anal. Chem.* **2009**, *81*, 9109–9113. [[CrossRef](#)] [[PubMed](#)]
6. Catanante, G.; Mishra, R.K.; Hayat, A.; Marty, J.-L. Sensitive analytical performance of folding based biosensor using methylene blue tagged aptamers. *Talanta* **2016**, *153*, 138–144. [[CrossRef](#)] [[PubMed](#)]
7. Yang, S.; Li, H.; Xu, L.; Deng, Z.; Han, W.; Liu, Y.; Jiang, W.; Zu, Y. Oligonucleotide aptamer-mediated precision therapy of hematological malignancies. *Mol. Ther. Nucleic Acids* **2018**, *13*, 164–175. [[CrossRef](#)]
8. Bernat, V.; Disney, M.D. RNA structures as mediators of neurological diseases and as drug targets. *Neuron* **2015**, *87*, 28–46. [[CrossRef](#)]
9. Villalonga, A.; Mayol, B.; Villalonga, R.; Vilela, D. Electrochemical aptasensors for clinical diagnosis. A review of the last five years. *Sens. Actuat. B Chem.* **2022**, *369*, 132318. [[CrossRef](#)]

10. Ikebukuro, K.; Kiyohara, C.; Sode, K. Electrochemical detection of protein using a double aptamer sandwich. *Anal. Lett.* **2004**, *37*, 2901–2909. [[CrossRef](#)]
11. Hianik, T.; Wang, J. Electrochemical aptasensors—Recent achievements and perspectives. *Electroanalysis* **2009**, *21*, 1223–1235. [[CrossRef](#)]
12. Abd-Ellatief, R.; Abd-Ellatief, M.R. Electrochemical aptasensors: Current status and future perspectives. *Diagnostics* **2021**, *11*, 104. [[CrossRef](#)]
13. Bard, A.J.; Faulkner, L.R.; White, H.S. *Electrochemical Methods: Fundamentals and Applications*, 3rd ed.; Wiley: Hoboken, NJ, USA, 2022; ISBN 9781119334071.
14. Girault, H.H. *Analytical and Physical Electrochemistry*, 1st ed.; EPFL Press: Lausanne, Switzerland, 2004; p. 315.
15. Renedo, O.D.; Alonso-Lomillo, M.A.; Martínez, M.J.A. Recent developments in the field of screen-printed electrodes and their related applications. *Talanta* **2007**, *73*, 202–219. [[CrossRef](#)] [[PubMed](#)]
16. García-Miranda Ferrari, A.; Rowley-Neale, S.J.; Banks, C.E. Screen-printed electrodes: Transitioning the laboratory in-to-the field. *Talanta Open* **2021**, *3*, 100032. [[CrossRef](#)]
17. Evtugyn, G.; Porfireva, A.; Shamagsumova, R.; Hianik, T. Advances in electrochemical aptasensors based on carbon nanomaterials. *Chemosensors* **2020**, *8*, 96. [[CrossRef](#)]
18. Lai, H.; Ming, P.; Wu, M.; Wang, S.; Sun, D.; Zhai, H. An electrochemical aptasensor based on P-Ce-MOF@MWCNTs as signal amplification strategy for highly sensitive detection of zearalenone. *Food Chem.* **2023**, *423*, 136331. [[CrossRef](#)]
19. Fujishima, A.; Honda, K. Electrochemical photolysis of water at a semiconductor electrode. *Nature* **1972**, *238*, 37–38. [[CrossRef](#)] [[PubMed](#)]
20. Bertel, L.; Miranda, D.A.; García-Martín, J.M. Nanostructured titanium dioxide surfaces for electrochemical biosensing. *Sensors* **2021**, *21*, 6167. [[CrossRef](#)]
21. Shetti, N.P.; Bukkitgar, S.D.; Reddy, K.R.; Reddy, C.V.; Aminabhavi, T.M. ZnO-based nanostructured electrodes for electrochemical sensors and biosensors in biomedical applications. *Biosens. Bioelectron.* **2019**, *141*, 111417. [[CrossRef](#)] [[PubMed](#)]
22. Bukkitgar, S.D.; Kumar, S.; Pratibha; Singh, S.; Singh, V.; Raghava Reddy, K.; Sadhu, V.; Bagihalli, G.B.; Shetti, N.P.; Venkata Reddy, C.; et al. Functional nanostructured metal oxides and its hybrid electrodes—Recent advancements in electrochemical biosensing applications. *Microchem. J.* **2020**, *159*, 105522. [[CrossRef](#)]
23. Song, J.; Lin, X.; Jiang, N.; Huang, M. Carbon-doped WO<sub>3</sub> electrochemical aptasensor based on Box-Behnken strategy for highly-sensitive detection of tetracycline. *Food Chem.* **2022**, *367*, 130564. [[CrossRef](#)]
24. Chen, X.; Yang, Z.; Ai, L.; Zhou, S.; Fan, H.; Ai, S. Signal-off photoelectrochemical aptasensor for *S. aureus* detection based on graphite-like carbon nitride decorated with nickel oxide. *Electroanalysis* **2022**, *34*, 310–315. [[CrossRef](#)]
25. Samie, H.A.; Arvand, M. Label-free electrochemical aptasensor for progesterone detection in biological fluids. *Bioelectrochemistry* **2020**, *133*, 107489. [[CrossRef](#)] [[PubMed](#)]
26. Mohan, S.; Srivastava, P.; Maheshwari, S.N.; Sundar, S.; Prakash, R. Nano-structured nickel oxide based DNA biosensor for detection of visceral leishmaniasis (Kala-azar). *Analyst* **2011**, *136*, 2845–2851. [[CrossRef](#)]
27. Georgakilas, V.; Perman, J.A.; Tucek, J.; Zboril, R. Broad family of carbon nanoallotropes: Classification, chemistry, and applications of fullerenes, carbon dots, nanotubes, graphene, nanodiamonds, and combined superstructures. *Chem. Rev.* **2015**, *115*, 4744–4822. [[CrossRef](#)]
28. Rahman, M.A.; Kumar, P.; Park, D.-S.; Shim, Y.-B. Electrochemical sensors based on organic conjugated polymers. *Sensors* **2008**, *8*, 118–141. [[CrossRef](#)]
29. Hopkins, J.; Fidanovski, K.; Lauto, A.; Mawad, D. All-organic semiconductors for electrochemical biosensors: An overview of recent progress in material design. *Front. Bioeng. Biotechnol.* **2019**, *7*, 237. [[CrossRef](#)]
30. Kim, K.; Yoo, H.; Lee, E.K. New opportunities for organic semiconducting polymers in biomedical applications. *Polymers* **2022**, *14*, 2960. [[CrossRef](#)] [[PubMed](#)]
31. Hirsch, A. The era of carbon allotropes. *Nat. Mater.* **2010**, *9*, 868–871. [[CrossRef](#)]
32. Yang, X.; Ebrahimi, A.; Li, J.; Cui, Q. Fullerene-biomolecule conjugates and their biomedical applications. *Int. J. Nanomed.* **2014**, *9*, 77–92. [[CrossRef](#)]
33. Pilehvar, S.; De Wael, K. Recent advances in electrochemical biosensors based on fullerene-C60 nano-structured platforms. *Biosensors* **2015**, *5*, 712–735. [[CrossRef](#)]
34. Bardhan, N.M. 30 years of advances in functionalization of carbon nanomaterials for biomedical applications: A practical review. *J. Mater. Res.* **2017**, *32*, 107–127. [[CrossRef](#)]
35. Thirumalraj, B.; Palanisamy, S.; Chen, S.-M.; Lou, B.-S. Preparation of highly stable fullerene C60 decorated graphene oxide nanocomposite and its sensitive electrochemical detection of dopamine in rat brain and pharmaceutical samples. *J. Colloid Interface Sci.* **2016**, *462*, 375–381. [[CrossRef](#)] [[PubMed](#)]
36. Compton, R.G.; Spackman, R.A.; Wellington, R.G.; Green, M.L.H.; Turner, J. A C60 modified electrode: Electrochemical formation of tetra-butylammonium salts of C60 anions. *J. Electroanal. Chem.* **1992**, *327*, 337–341. [[CrossRef](#)]
37. Cassell, A.M.; Scrivens, W.A.; Tour, J.M. Assembly of DNA/fullerene hybrid materials. *Angew. Chem. Int. Ed. Engl.* **1998**, *37*, 1528–1531. [[CrossRef](#)]

38. Bai, L.; Chen, Y.; Bai, Y.; Chen, Y.; Zhou, J.; Huang, A. Fullerene-doped polyaniline as new redox nanoprobe and catalyst in electrochemical aptasensor for ultrasensitive detection of *Mycobacterium tuberculosis* MPT64 antigen in human serum. *Biomaterials* **2017**, *133*, 11–19. [[CrossRef](#)]
39. Ferrier, D.C.; Honeychurch, K.C. Carbon nanotube (CNT)-based biosensors. *Biosensors* **2021**, *11*, 486. [[CrossRef](#)]
40. Hianik, T. Aptamer-based biosensors. In *Encyclopedia of Interfacial Chemistry: Surface Science and Electrochemistry*; Wandelt, K., Ed.; Elsevier: Amsterdam, The Netherlands, 2018; Volume 7, pp. 11–19.
41. Hianik, T.; Porfireva, A.; Grman, I.; Evtugyn, G. EQCM biosensors based on DNA aptamers and antibodies for rapid detection of prions. *Protein Pept. Lett.* **2009**, *16*, 363–367. [[CrossRef](#)] [[PubMed](#)]
42. Miodek, A.; Castillo, G.; Hianik, T.; Korri-Youssoufi, H. Electrochemical aptasensor of human cellular prion based on multiwalled carbon nanotubes modified with dendrimers: A platform for connecting redox markers and aptamers. *Anal. Chem.* **2013**, *85*, 7704–7712. [[CrossRef](#)]
43. Miodek, A.; Castillo, G.; Hianik, T.; Korri-Youssoufi, H. Electrochemical aptasensor of cellular prion protein based on modified polypyrrole with redox dendrimers. *Biosens. Bioelectron.* **2014**, *56*, 104–111. [[CrossRef](#)]
44. Li, Y.; Hua, X.; Wang, J.; Jin, B. cMWCNT/CoHCF/AuNPs nanocomposites aptasensor for electrochemical detection of interleukin-6. *Talanta Open* **2023**, *7*, 100188. [[CrossRef](#)]
45. Cao, S.; Zhao, H.; Chen, K.; Zhou, F.; Lan, M. An electrochemical aptasensor based on multi-walled carbon nanotubes loaded with PtCu nanoparticles as signal label for ultrasensitive detection of adenosine. *Anal. Chim. Acta* **2023**, *1260*, 341212. [[CrossRef](#)] [[PubMed](#)]
46. Zelada-Guillén, G.A.; Riu, J.; Düzgün, A.; Rius, F.X. Immediate detection of living bacteria at ultralow concentrations using a carbon nanotube based potentiometric aptasensor. *Angew. Chem. Int. Ed. Engl.* **2009**, *48*, 7334–7337. [[CrossRef](#)] [[PubMed](#)]
47. Zelada-Guillén, G.A.; Blondeau, P.; Rius, F.X.; Riu, J. Carbon nanotube-based aptasensors for the rapid and ultrasensitive detection of bacteria. *Methods* **2013**, *63*, 233–238. [[CrossRef](#)] [[PubMed](#)]
48. Hasan, M.R.; Pulingam, T.; Appaturi, J.N.; Zifruddin, A.N.; Teh, S.J.; Lim, T.W.; Ibrahim, F.; Leo, B.F.; Thong, K.L. Carbon nanotube-based aptasensor for sensitive electrochemical detection of whole-cell *Salmonella*. *Anal. Biochem.* **2018**, *554*, 34–43. [[CrossRef](#)] [[PubMed](#)]
49. Zou, Y.; Griveau, S.; Ringuedé, A.; Bedioui, F.; Richard, C.; Slim, C. Functionalized multi-walled carbon nanotube-based aptasensors for diclofenac detection. *Front. Chem.* **2021**, *9*, 812909. [[CrossRef](#)]
50. Wang, Y.; Gong, C.; Zhu, Y.; Wang, Q.; Geng, L. Signal-on electrochemical aptasensor for sensitive detection of sulfamethazine based on carbon quantum dots/tungsten disulfide nanocomposites. *Electrochim. Acta* **2021**, *393*, 139054. [[CrossRef](#)]
51. Cheng, W.; Pan, J.; Yang, J.; Zheng, Z.; Lu, F.; Chen, Y.; Gao, W. A photoelectrochemical aptasensor for thrombin based on the use of carbon quantum dot-sensitized TiO<sub>2</sub> and visible-light photoelectrochemical activity. *Microchim. Acta* **2018**, *185*, 263. [[CrossRef](#)]
52. Kulikova, T.; Gorbachuk, V.; Stoikov, I.; Rogov, A.; Evtugyn, G.; Hianik, T. Impedimetric determination of kanamycin in milk with aptasensor based on carbon black-oligolactide composite. *Sensors* **2020**, *20*, 4738. [[CrossRef](#)]
53. Song, H.; Zhang, Y.; Wang, S.; Huang, K.; Luo, Y.; Zhang, W.; Xu, W. Label-free polygonal-plate fluorescent-hydrogel biosensor for ultrasensitive microRNA detection. *Sens. Actuators B Chem.* **2020**, *306*, 127554. [[CrossRef](#)]
54. Hernández-Cancel, G.; Suazo-Dávila, D.; Medina-Guzmán, J.; Rosado-González, M.; Díaz-Vázquez, L.M.; Griebenow, K. Chemically glycosylation improves the stability of an amperometric horseradish peroxidase biosensor. *Anal. Chim. Acta* **2015**, *854*, 129–139. [[CrossRef](#)] [[PubMed](#)]
55. Visa, M.; Andronic, L.; Enesca, A. Behavior of the new composites obtained from fly ash and titanium dioxide in removing of the pollutants from wastewater. *Appl. Surf. Sci.* **2016**, *388*, 359–369. [[CrossRef](#)]
56. Şerban, I.; Enesca, A. Metal oxides-based semiconductors for biosensors applications. *Front. Chem.* **2020**, *8*, 354. [[CrossRef](#)]
57. Ma, X.; Li, X.; Zhang, W.; Meng, F.; Wang, X.; Qin, Y.; Zhang, M. Carbon-based nanocomposite smart sensors for the rapid detection of mycotoxins. *Nanomaterials* **2021**, *11*, 2851. [[CrossRef](#)]
58. Nadzirah, S.; Azizah, N.; Hashim, U.; Gopinath, S.C.B.; Kashif, M. Titanium dioxide nanoparticle-based interdigitated electrodes: A novel current to voltage DNA biosensor recognizes *E. coli* O157:H7. *PLoS ONE* **2015**, *10*, e0139766. [[CrossRef](#)]
59. Karimipour, M.; Heydari-Bafrooei, E.; Sanjari, M.; Johansson, M.B.; Molaei, M. A glassy carbon electrode modified with TiO<sub>2</sub>(200)-rGO hybrid nanosheets for aptamer based impedimetric determination of the prostate specific antigen. *Mikrochim. Acta* **2018**, *186*, 33. [[CrossRef](#)] [[PubMed](#)]
60. Muniandy, S.; Teh, S.J.; Appaturi, J.N.; Thong, K.L.; Lai, C.W.; Ibrahim, F.; Leo, B.F. A reduced graphene oxide-titanium dioxide nanocomposite based electrochemical aptasensor for rapid and sensitive detection of *Salmonella enterica*. *Bioelectrochemistry* **2019**, *127*, 136–144. [[CrossRef](#)] [[PubMed](#)]
61. Zhang, Z.; Zhang, S.; He, L.; Peng, D.; Yan, F.; Wang, M.; Zhao, J.; Zhang, H.; Fang, S. Feasible electrochemical biosensor based on plasma polymerization-assisted composite of polyacrylic acid and hollow TiO<sub>2</sub> spheres for sensitively detecting lysozyme. *Biosens. Bioelectron.* **2015**, *74*, 384–390. [[CrossRef](#)]
62. Erdem, A.; Eksin, E.; Muti, M. Chitosan–graphene oxide based aptasensor for the impedimetric detection of lysozyme. *Coll. Surf. B: Biointerfaces* **2014**, *115*, 205–211. [[CrossRef](#)]

63. Wang, X.; Qin, Y.; Zhang, X.; Leng, Y.; Chen, Z. Au/TiO<sub>2</sub> nanorod arrays-based electrochemical aptasensor for ultrasensitive detection of adenosine. *Microchem. J.* **2023**, *190*, 108695. [[CrossRef](#)]
64. Evtugyn, G.; Cherkina, U.; Porfireva, A.; Danzberger, J.; Ebner, A.; Hianik, T. Electrochemical aptasensor based on ZnO modified gold electrode. *Electroanalysis* **2013**, *25*, 1855–1863. [[CrossRef](#)]
65. Zhang, S.; Wang, Y.; Sheng, Q.; Yue, T. Electrochemical aptasensor based on ZnO-Au nanocomposites for the determination of ochratoxin A in wine and beer. *Processes* **2023**, *11*, 864. [[CrossRef](#)]
66. Rahimi, F.; Roshanfekar, H.; Peyman, H. Ultra-sensitive electrochemical aptasensor for label-free detection of Aflatoxin B1 in wheat flour sample using factorial design experiments. *Food Chem.* **2021**, *343*, 128436. [[CrossRef](#)] [[PubMed](#)]
67. Grabowska, I.; Hepel, M.; Kurzątkowska-Adaszyńska, K. Advances in design strategies of multiplex electrochemical aptasensors. *Sensors* **2021**, *22*, 161. [[CrossRef](#)] [[PubMed](#)]
68. Evtugyn, G.; Belyakova, S.; Porfireva, A.; Hianik, T. Electrochemical aptasensors based on hybrid metal-organic frameworks. *Sensors* **2020**, *20*, 6963. [[CrossRef](#)]
69. Hansen, J.A.; Wang, J.; Kawde, A.-N.; Xiang, Y.; Gothelf, K.V.; Collins, G. Quantum-dot/aptamer-based ultrasensitive multi-analyte electrochemical biosensor. *J. Am. Chem. Soc.* **2006**, *128*, 2228–2229. [[CrossRef](#)]
70. Pavel, I.-A.; Lakard, S.; Lakard, B. Flexible sensors based on conductive polymers. *Chemosensors* **2022**, *10*, 97. [[CrossRef](#)]
71. Fan, X.; Nie, W.; Tsai, H.; Wang, N.; Huang, H.; Cheng, Y.; Wen, R.; Ma, L.; Yan, F.; Xia, Y. PEDOT:PSS for flexible and stretchable electronics: Modifications, strategies, and applications. *Adv. Sci.* **2019**, *6*, 1900813. [[CrossRef](#)]
72. Malinauskas, A. Self-doped polyanilines. *J. Power Sources* **2004**, *126*, 214–220. [[CrossRef](#)]
73. Yen, Y.-K.; Chao, C.-H.; Yeh, Y.-S. A Graphene-PEDOT:PSS modified paper-based aptasensor for electrochemical impedance spectroscopy detection of tumor marker. *Sensors* **2020**, *20*, 1372. [[CrossRef](#)]
74. Liu, S.; Xing, X.; Yu, J.; Lian, W.; Li, J.; Cui, M.; Huang, J. A novel label-free electrochemical aptasensor based on graphene-polyaniline composite film for dopamine determination. *Biosens. Bioelectron.* **2012**, *36*, 186–191. [[CrossRef](#)] [[PubMed](#)]
75. Jolly, P.; Miodek, A.; Yang, D.-K.; Chen, L.-C.; Lloyd, M.D.; Estrela, P. Electro-engineered polymeric films for the development of sensitive aptasensors for prostate cancer marker detection. *ACS Sens.* **2016**, *1*, 1308–1314. [[CrossRef](#)]
76. Šafaříková, E.; Švihálková, Š.L.; Štriteský, S.; Kubala, L.; Vala, M.; Weiter, M.; Vítěček, J. Evaluation and improvement of organic semiconductors' biocompatibility towards fibroblasts and cardiomyocytes. *Sens. Actuators B Chem.* **2018**, *260*, 418–425. [[CrossRef](#)]
77. Haya, G.; Runsewe, D.O.; Otakpor, M.U.; Pohlman, G.E.; Towne, A.; Betancourt, T.; Irvin, J.A. Functionalized thiophene-based aptasensors for the electrochemical detection of Mucin-1. *ACS Appl. Polym. Mater.* **2023**, *5*, 1208–1218. [[CrossRef](#)]
78. Barsan, M.M.; Ghica, M.E.; Brett, C.M.A. Electrochemical sensors and biosensors based on redox polymer/carbon nanotube modified electrodes: A review. *Anal. Chim. Acta* **2015**, *881*, 1–23. [[CrossRef](#)] [[PubMed](#)]
79. Smolko, V.; Shurpik, D.; Porfireva, A.; Evtugyn, G.; Stoikov, I.; Hianik, T. Electrochemical aptasensor based on Poly(Neutral Red) and carboxylated Pillar [5]arene for sensitive determination of Aflatoxin M1. *Electroanalysis* **2018**, *30*, 486–496. [[CrossRef](#)]
80. Goida, A.; Kuzin, Y.; Evtugyn, V.; Porfireva, A.; Evtugyn, G.; Hianik, T. Electrochemical sensing of idarubicin—DNA interaction using electropolymerized azure B and methylene blue mediation. *Chemosensors* **2022**, *10*, 33. [[CrossRef](#)]
81. Appaturi, J.N.; Pulingam, T.; Thong, K.L.; Muniandy, S.; Ahmad, N.; Leo, B.F. Rapid and sensitive detection of *Salmonella* with reduced graphene oxide-carbon nanotube based electrochemical aptasensor. *Anal. Biochem.* **2020**, *589*, 113489. [[CrossRef](#)]
82. Jia, F.; Duan, N.; Wu, S.; Dai, R.; Wang, Z.; Li, X. Impedimetric *Salmonella* aptasensor using a glassy carbon electrode modified with an electrodeposited composite consisting of reduced graphene oxide and carbon nanotubes. *Microchim. Acta* **2016**, *183*, 337–344. [[CrossRef](#)]
83. Kumar, V.; Shorie, M.; Ganguli, A.K.; Sabherwal, P. Graphene-CNT nanohybrid aptasensor for label free detection of cardiac biomarker myoglobin. *Biosens. Bioelectron.* **2015**, *72*, 56–60. [[CrossRef](#)]
84. Beiki, T.; Najafpour-Darzi, G.; Mohammadi, M.; Shakeri, M.; Boukherroub, R. Fabrication of a novel electrochemical biosensor based on a molecular imprinted polymer-aptamer hybrid receptor for lysozyme determination. *Anal. Bioanal. Chem.* **2022**, *415*, 899–911. [[CrossRef](#)] [[PubMed](#)]
85. Akbarzadeh, S.; Khajehsharifi, H.; Hajihosseini, S. Detection of oxytetracycline using an electrochemical label-free aptamer-based biosensor. *Biosensors* **2022**, *12*, 468. [[CrossRef](#)] [[PubMed](#)]
86. Tian, J.; Huang, T.; Jusheng Lu, J. Photoelectrochemical aptasensor for mucin 1 based on DNA/aptamer linking of quantum dots and TiO<sub>2</sub> nanotube arrays. *Anal. Meth.* **2016**, *8*, 2375–2382. [[CrossRef](#)]
87. Majd, S.M.; Mirzapour, F.; Shamsipur, M.; Manouchehri, I.; Babaee, E.; Pashabadi, A.; Moradian, R. Design of a novel aptamer/molecularly imprinted polymer hybrid modified Ag–Au@Insulin nanoclusters/Au-gate-based MoS<sub>2</sub> nanosheet field-effect transistor for attomolar detection of BRCA1 gene. *Talanta* **2023**, *257*, 124394. [[CrossRef](#)]
88. Rauf, S.; Tayyab, Z.; Pan, X.; Yang, Y.; Hussain, A.; Yunzhi, H.; Amin, N.; Rauf, S.; Salem, A.; Xu, W. Highly electroactive Sb-doped BaSrFeO<sub>3-d</sub> semiconductor as a label-free electrochemical aptasensing platform for thrombin detection. *IEEE Sens. J.* **2023**, *23*, 9077–9085. [[CrossRef](#)]
89. Vasudevan, M.; Remesh, S.; Perumal, V.; Raja, P.B.; Ibrahim, M.N.M.; Gopinath, S.C.B.; Karuppanan, S.; Ovinis, M. Facile synthesis of MoS<sub>2</sub> nanoflower-Ag NPs grown on lignin-derived graphene for Troponin I aptasensing. *Chem. Eng. J.* **2023**, *468*, 143613. [[CrossRef](#)]

90. Cheng, S.; Zhang, H.; Huang, J.; Xu, R.; Suna, X.; Guo, Y. Highly sensitive electrochemiluminescence aptasensor based on dual-signal amplification strategy for kanamycin detection. *Sci. Total Environ.* **2020**, *737*, 139785. [[CrossRef](#)] [[PubMed](#)]
91. Mehlhorn, A.; Rahimi, P.; Joseph, Y. Aptamer-based biosensors for antibiotic detection: A review. *Biosensors* **2018**, *8*, 54. [[CrossRef](#)] [[PubMed](#)]

**Disclaimer/Publisher's Note:** The statements, opinions and data contained in all publications are solely those of the individual author(s) and contributor(s) and not of MDPI and/or the editor(s). MDPI and/or the editor(s) disclaim responsibility for any injury to people or property resulting from any ideas, methods, instructions or products referred to in the content.